

P465L ppar γ mutation confers partial resistance to the hypolipidemic action of fibrates.

Journal:	<i>Diabetes, Obesity and Metabolism</i>
Manuscript ID	DOM-18-0100-OP.R1
Manuscript Type:	Original Paper
Date Submitted by the Author:	n/a
Complete List of Authors:	Rodriguez-Cuenca, Sergio; University of Cambridge, Wellcome Trust MRC Institute of Metabolic Sciences Carobbio, Stefania; University of Cambridge, Wellcome Trust MRC Institute of Metabolic Sciences; Wellcome Trust Sanger Institute, Wellcome Trust Genome Campus, Barcelo-Coblijn, Gwendolyn ; 3 Institut d'Investigació Sanitària Illes Balears (IdISBa, Balearic Islands Health Research Institute), Prieur, Xavier; Universite de Nantes, L'Institut du Thorax, INSERM, CNRS Relat, Joana; University of Barcelona, Department of Nutrition, Food Science and Gastronomy, School of Pharmacy and Food Science, Food and Nutrition Torribera Campus; Institute of Biomedicine of the University of Barcelona Amat, Ramon; Universitat Pompeu Fabra (UPF), Cell Signaling Unit, Departament de Ciències Experimentals i de la Salut Campbell, Mark; University of Cambridge, Wellcome Trust MRC Institute of Metabolic Sciences Dias, Ana Rita; University of Cambridge, Wellcome Trust MRC Institute of Metabolic Sciences Bahri, Myriam; University of Cambridge, Wellcome Trust MRC Institute of Metabolic Sciences; Wellcome Trust Sanger Institute, Wellcome Trust Genome Campus, Gray, Sarah; University of Northern British Columbia, Northern Medical Program Vidal-Puig, Antonio; University of Cambridge, Wellcome Trust MRC Institute of Metabolic Sciences
Key Words:	mouse model, dyslipidaemia, lipid-lowering therapy, liver, insulin resistance, body composition

1
2
3
4
5
6
7 **P465L ppar γ mutation confers partial resistance to the hypolipidemic**
8 **action of fibrates .**
9

10
11 **Sergio Rodriguez-Cuenca^{1*}, Stefania Carobbio^{1,2*}, Gwendolyn Barceló-Coblijn³, Xavier**
12 **Prieur⁴, Joana Relat^{5,6}, Ramon Amat⁷, Mark Campbell¹, Ana Rita Dias¹, Myriam Bahri^{1,2},**
13 **Sarah L. Gray⁸, and Antonio Vidal-Puig^{1,2}.**
14
15

16
17 ¹ University of Cambridge Metabolic. Research Laboratories, Level 4, Wellcome Trust-MRC
18 Institute of Metabolic Science, Cambridge, UK.
19

20 ² Wellcome Trust Sanger Institute, Wellcome Trust Genome Campus, Hinxton, Cambridge, UK.
21

22 ³ Institut d'Investigació Sanitària Illes Balears (IdISBa, Balearic Islands Health Research Institute),
23 Palma, Balearic Islands, Spain.
24

25 ⁴ L'Institut du Thorax, INSERM, CNRS, Université de Nantes, Nantes, France.
26

27 ⁵ Department of Nutrition, Food Science and Gastronomy, School of Pharmacy and Food Science,
28 Food and Nutrition Torribera Campus. University of Barcelona (UB), Santa Coloma de Gramenet
29 (Spain); INSA-UB, Nutrition and Food Safety Research Institute, University of Barcelona,
30 Barcelona, Spain..
31

32 ⁶ Institute of Biomedicine of the University of Barcelona (IBUB), Barcelona, Spain.
33

34 ⁷ Cell Signaling Unit, Departament de Ciències Experimentals i de la Salut, Universitat Pompeu
35 Fabra (UPF), Barcelona, Spain.
36

37 ⁸ University of Northern British Columbia, Northern Medical Program, 3333 University Way,
38 Prince George, BC, V2N 4Z9, Canada.
39

40 *These authors contributed equally to this work
41

42 **CORRESPONDING AUTHORS EMAIL:**

43 sr441@medschl.cam.ac.uk; sc547@medschl.cam.ac.uk; ajv22@medschl.cam.ac.uk
44

45 **RUNNING TITLE: P465L ppar γ mutation impairs ppar α function.**
46

47 **Word count:**

48 **Number of Figures: 5**
49
50
51
52
53
54

Abstract:

Familial partial lipodystrophic syndrome 3 (FPLD3) is associated with mutations in the transcription factor PPAR γ . One of these mutations, the P467L, confers a dominant negative effect. We and others have previously investigated the pathophysiology associated to this mutation using a humanised mouse model that recapitulates most of the clinical symptoms observed in patients when phenotyped under different experimental conditions. One of the key clinical manifestations observed both, in humans and mouse models, is the ectopic accumulation of fat in the liver. Here, we dissect the molecular mechanisms that contribute to the excessive accumulation of lipids in the liver and characterise the negative effect of this PPAR γ mutation on the activity of PPAR α *in vivo* when activated by fibrates. P465L mice have increased levels of insulin and free fatty acids (FFA), exhibit decreased levels of Very Low Density Lipoproteins (VLDL) when fed high fat diet (HFD) and a partial impaired response to the hypolipidemic action of WY14643. This indicates that the deleterious effects of P465L-PPAR γ mutation may be magnified by their collateral negative effect on PPAR α function.

KEYWORDS: lipodystrophy, fatty liver, P465L ppar-gamma, ppar-alpha, fibrates.

Introduction:

Peroxisome proliferator-activated receptors (PPARs) are nuclear receptors that regulate energy homeostasis and coordinate biochemical processes involved in anabolic and catabolic processes. This family of transcription factors comprises three members: PPAR γ (with two isoforms: PPAR γ 1 and PPAR γ 2), PPAR α and PPAR δ [1].

PPAR γ regulates adipose tissue development and expansion, and harmonises the functional balance between lipogenic and lipolytic programmes [2]. Genetic defects in PPAR γ cause severe metabolic lipodystrophy phenotypes [3] known as familial partial lipodystrophy syndrome type III (FPLD3) [4]. Amongst patients suffering this syndrome, those carrying the P467L mutation (rs121909244) exhibit a lipodystrophic phenotype, hypertension, hyperglycemia, hepatic steatosis, and severe dyslipidemia, a complex phenotype that is partially recapitulated in the humanised P465L-PPAR γ mutant mouse under different nutritional and genetically induced challenges such as HFD feeding and backcrossed into ob/ob, apolipoprotein E knockout (APOEKO) and Akita murine genetic backgrounds [5-7]. The isoform PPAR γ 2 is, under physiological conditions, preferentially expressed in WAT and BAT. Other organs such as liver, predominantly express the PPAR γ 1 isoform, but can, under pathological conditions such as overnutrition and obesity, induce *de novo* the expression of the PPAR γ 2 isoform [8]. This indicates that the types and relative amounts of PPARs coexisting in the same cell/tissue under specific physiological and pathophysiological conditions varies according to specific nutritional status and metabolic adaptations.

PPAR α is another important member of the PPAR family, which plays a fundamental role in lipid oxidation and biosynthesis, gluconeogenesis, cholesterol catabolism and ketogenesis [9]. PPAR α is detected in tissues characterised by high rates of β -oxidation such as heart, skeletal muscle, and liver [10]. Conversely, genetic ablation of PPAR α in mice has confirmed its preferential involvement in fatty acid oxidation and that when PPAR α is dysfunctional, it causes hepatic steatosis [11] and severe fasting hypoglycaemia [12]. According to the role of PPAR α

1
2
3
4
5
6
7 controlling fatty acid metabolism, fibrates, a class of synthetic PPAR α ligands, exert beneficial
8 metabolic effects in patients with metabolic syndrome and in rodent models of obesity, insulin
9 resistance and diabetes. For instance, a well-established fibrate, WY14643 (pirinixic acid),
10 decreases plasma triglycerides, reduces adiposity, and improves hepatic steatosis and insulin
11 sensitivity in lipoatrophic mice [13].
12
13
14

15
16 Given that PPARs share common co-activators, co-repressors and partners as well as DNA
17 responsive elements (PPRE), we hypothesised that the changes in expression patterns or activity of
18 PPARs may affect the transactivation capacity of the members of the family. *In vitro* evidence
19 indicates that PPARs exhibit promiscuity in their binding to specific coactivators/corepressors
20 known to be involved in complex functional crosstalks. This has been partially addressed *in vitro* by
21 showing that mutants for PPAR α such as a dominant negative [14] or a ligand binding domain
22 lacking mutant [15] exert cross-inhibition of the wild type (WT) form of PPAR α , and also of
23 PPAR γ and PPAR δ , by competition for coactivators [14]. Similarly, several PPAR γ dominant
24 negative mutants have been shown to repress the activity of PPAR α *in vitro* [14, 16].
25
26
27
28
29
30
31
32

33 The P467L PPAR γ mutation exerts a dominant negative effect on WT PPAR γ *in vitro* by
34 reducing the promoter turnover rate and out-compete the WT receptor for promoter binding sites
35 and also attenuating the release of corepressor and recruitment coactivator [17-20]. The
36 pathophysiological relevance of this crosstalk between PPARs *in vivo* has not been studied.
37
38
39

40 Our laboratory has previously shown that the humanised murine model P465L PPAR γ
41 developed hepatic steatosis after four months on HFD [5] in the same way that P467L human
42 carriers do [21]. Here, we dissect the mechanisms leading to this phenotype *in vivo* and propose that
43 the P465L PPAR γ mutation increases susceptibility to fatty liver through a mechanism involving a
44 partial deficiency of the transactivation capacity of PPAR α . We found that the P465L mice have
45 increased levels of insulin and FFA, both risk factors associated to fatty liver; The P465L mice also
46 display decreased levels of VLDL when fed HFD and partial impaired response to the
47
48
49
50
51
52
53

1
2
3
4
5
6
7 hypolipidemic action of WY14643. Moreover, gene expression profiling revealed that P465L
8 PPAR γ negatively impacts on the transcriptional activation and repression mediated by PPAR α
9 agonists in a variety of metabolic pathways.
10
11
12
13

14 **Material and Methods:**

15
16 **Animals.** P465L/+ PPAR γ mice were generated as described previously [5]. All animals used in
17 this study were fed a standard chow or HFD (45%Kcal from fat) *ad libitum* and housed at 24°C
18 with 12h light cycle. The mice were divided into groups of 7-8 mice. For both genotypes, mice were
19 distributed into the following groups: chow diet/vehicle, chow diet/WY14643; HFD/vehicle and
20 HFD/WY14643. Feeding of HFD started when the mice were 5w old for a period of 28d. Then,
21 mice were injected intraperitoneally with vehicle or WY14643 (25mg/kg/day) for 5d. Additionally,
22 we used WT and P465L fed chow and HFD (45%Kcal from fat) for a period of 12 weeks and cull
23 them in fed and fasting conditions (overnight).
24
25
26
27
28
29
30

31 This research was regulated under the Animals (Scientific Procedures) Act 1986 Amendment
32 Regulations 2012 following ethical review by the University of Cambridge, Animal Welfare and
33 Ethical Review Body (AWERB).
34
35

36 **Blood biochemistry.** Enzymatic assay kits were used for determination of plasma free fatty acids
37 (Roche), triglycerides (Siemens), glucose, and insulin (MesoScale discovery) according to
38 manufacturer's instructions.
39
40
41

42 **Liver triglycerides content.** Hepatic lipid content was measured following Folch method as
43 described previously [22].
44

45 **Lipoprotein separation by Fast protein liquid chromatography (FPLC).** Pooled plasma of each
46 experimental group was used for the isolation of lipoproteins using FPLC according to the
47 following online protocol from the *Diabetic Complications Consortium*.
48
49
50

51 <https://www.diacomp.org/shared/document.aspx?id=14&docType=Protocol>.

52 **Glycogen determination.** Hepatic glycogen content was measured as described previously [23].
53
54

1
2
3
4
5
6
7 **Histology.** The livers were dissected and fixed in 10% formalin, then they were cryoprotected (20%
8 sucrose) and frozen in chilled isopentane prior to sectioning using a cryostat. Cryosectioned tissue
9 was stained for lipid with Oil Red O.

10
11
12 **Lipid analysis.** Liver tissue was homogenized with a tissue blender. Lipids were extracted using n-
13 hexane/2-propanol. Tissue extracts were centrifuged at 1,000g to pellet debris. The lipid-containing
14 organic phase was decanted and stored under nitrogen at -80°C until analysis [24, 25]. Total lipids
15 were subjected to base catalyzed transesterification, converting the acyl chains to fatty acid methyl
16 esters (FAME) [26]. Heptadecanoic acid (17:0) was used as the internal standard. Individual
17 FAMES were separated by gas liquid chromatography using a SP-2330 column (0.32 mm ID, 30 m
18 length) and a gas chromatograph equipped with dual autosamplers and dual flame ionization
19 detectors. The SCD1 (Stearoyl-CoA desaturase (Δ -9-desaturase)) index is the ratio of products
20 (16:1n-7 and 18:1n-9) to precursors (16:0 and 18:0) fatty acids. The ELOVL6 (Fatty Acid Elongase
21 6) index is the ratio of products (18:0, 18:1n-7 and 18:1n-9) to precursors (16:0 and 16:1n-7) fatty
22 acids; the FADS1 (fatty acid desaturase 1) index was measured as the ratio (20:4n6/20:3n6) and the
23 FADS2 (fatty acid desaturase 2) index was obtained from the (20:3n-6)/(18:2n-6) ratio.

24
25
26
27
28
29
30
31
32
33
34 **Retrotranscription and Real-Time PCR analysis.** RNA was extracted from 50mg of liver using
35 the Trizol reagent in accordance with manufacturer's instructions. $1\mu\text{g}$ of RNA was converted to
36 cDNA using M-MLV Reverse Transcriptase, 100ng random hexamers and 1mM dNTPs in a final
37 volume of $20\mu\text{L}$. Real-Time PCR was performed using SybrGreen primers (250nmol) or Taqman
38 primers and probes. The reactions were carried out using specific ABI Master Mixes in a 7900HT
39 Fast Real-Time PCR System with 384-Well Block Module. Primers were designed using either
40 Primer Express 2.0 or Primer Blast software (<https://www.ncbi.nlm.nih.gov/tools/primer-blast/>). Sequences
41 are available at <http://tvp.mrl.ims.cam.ac.uk/primer-database-pagemax>. The geometrical average of four
42 different genes (β 2 microglobulin, β -actin, 18S and 36B4) was used as an internal control following
43 an already described normalization method [27]. HeatMaps were generated with the free software
44 Multiple Experiment Viewer-MeV- (<http://mev.tm4.org/>).

1
2
3
4
5
6
7
8
9
10
11
12
13
14
15
16
17
18
19
20
21
22
23
24
25
26
27
28
29
30
31
32
33
34
35
36
37
38
39
40
41
42
43
44
45
46
47
48
49
50
51
52
53
54
55
56
57
58
59
60

Western Blotting. Protein lysates from liver (50mg) were run in a NuPAGE™ 4-12% Bis-Tris Protein Gels and electrotransferred to a nitrocellulose membrane using a iBlot Dry Blotting System (ThermoFisher Scientific). All antibodies used were from Cell Signaling Technology apart from plin2/adrp, and anti-β-actin that were from abcam.

Statistical analysis. 2-way or 3-way ANOVA was used for the analysis of the interaction between genotype (G), diet (D) and treatment (T) for the fibrates intervention. Genotype (G), fasting (F) and/or diet (D) for the fasting cohort. IBM SPSS14 was used as statistical software.

For Review Only

Results

P465L PPAR γ mutant mice are hyperlipidemic and hyperinsulinemic.

P465L mutant mice showed higher levels of FFAs and TGs- and a tendency to increased cholesterol- in serum compared to WT mice (Fig1a), independently of the diet, and recapitulating the hyperlipidemia observed in the human carriers of the P467L mutation. Both, on chow diet or after a short challenge with HFD, P465L mice were normoglycemic in the presence of hyperinsulinemia (Fig1a) suggesting their insulin secretion was able to compensate for their peripheral insulin resistance; moreover, when challenged with HFD for a period of 12w, P465L mice became hyperglycemic (SFig1). The P465L mice also had increased hepatic glycogen levels in the chow fed state (SFig2a).

P465L PPAR γ mutant mice are resistant to the pro-lipolytic effect of WY14643 in adipose tissue.

WY14643 treatment increased plasma cholesterol levels in both genotypes as previously reported in other studies [28] and also increased levels of β -hydroxybutyrate (BHB) in both genotypes (Fig1a). The increase in BHB is compatible with fibrate mediated induction of hepatic β -oxidation, a response that was slightly increased (ns) in the P465L mice, particularly when fed HFD for 4w. Interestingly, when fasted o/n, the P465L mice showed significantly higher levels of BHB than WT mice (SFig1), reflecting an increase in hepatic FFA delivery and β -oxidation in P465L livers. At the organismal level, the acute treatment with WY14643 induced hepatomegaly in both genotypes, coupled to a specific decrease in the fat mass of WT mice (especially in gWAT) but not in P465L mice fed on HFD (Fig1b and SFig2). This differences in fat mass suggested that the P465L mutation may confer some degree of resistance against the pro-lipolytic effect of fibrates in adipose tissue [29].

P465L PPAR γ mutation promotes fatty liver and alterations in lipoprotein metabolism.

1
2
3
4
5
6
7 We have previously reported that P465L mice showed increased liver mass and hepatic
8 accumulation of TG content when fed HFD for 16w or when backcrossed with the ob/ob mouse [5].
9
10 In this new cohort of mice fed HFD for only 28d, the levels of hepatic TGs in P465L were already
11 marginally higher (ns) than WT mice (Fig2a). Unexpectedly, when mice fed on a HFD were treated
12 with fibrates we observed an increased hepatic fat content in P465L but not in WT mice (Fig2a).
13
14 The analysis of macrovacuoles in HFD fed animals revealed a decreased in WT treated with fibrates
15 but not in the P465L mice evidencing a degree of resistance to the hypolipidemic action of fibrates
16 (data not shown). In a similar line of evidence, P465L mice also presented more hepatic fat content
17 after o/n fasting than their WT controls, further indicating that a large amount of the fat
18 accumulated in the liver originated from adipose tissue (transient steatosis) (SFig1). Overall, these
19 data reinforced the hypothesis that PPAR α activated mechanisms (e.g. by response to
20 fibrates/fasting) regulating storage, oxidation and/or release of hepatic lipids were defective in
21 P465L mice.
22
23
24
25
26
27
28
29
30

31 **P465L PPAR γ increases hepatic MUFA/PUFA ratio.**

32
33 We next analysed the chemical characteristics of hepatic fatty acid (Fig2b). On a HFD, the
34 liver of P465L mice showed increased levels of monounsaturated fatty acids (MUFA). This was
35 associated with an increased SCD1 index (SFig2b) and active conversion of saturated (SFA) into
36 MUFA, the preferred FA substrate for triglyceride storage. Despite the increase in the SCD1 index,
37 the *scd1* and *scd2* mRNA levels were downregulated, revealing a mismatch between enzymatic flux
38 and gene regulation. The lower content of polyunsaturated fatty acids (PUFA) percentage in the
39 livers of HFD fed P465L mice was accounted for by reduced levels of 20:5 n-3, 22:5 n-3, 22:6 n-3
40 and 20:3 n-6 and 20:4 n-6 but not of 18:2 n-6 whose levels were increased in P465L, indicating an
41 impairment in the biosynthesis of PUFAs. Of relevance Gene expression profiles did not reveal
42 changes in the expression of elongases and fatty acid desaturases between genotypes (Fig2c);
43 however, the FADS1 index was downregulated in P465L livers. Interestingly, the FADS2 index
44 was significantly increased in WT mice treated with WY14643 but to a lesser extend in P465L mice
45
46
47
48
49
50
51
52
53
54

1
2
3
4
5
6
7 (SFig2b). Interestingly, the expression of *fads3*, a putative desaturase associated with changes in
8 PUFA levels [30], was downregulated in P465L livers (Fig2c), suggesting that FADS3 may be a
9 new fatty acid desaturase under the transcriptional regulation of PPAR γ . Gene expression profiling
10 of genes and analysis of proteins involved in *de novo* lipogenesis evidenced an increase in their
11 expression/levels in response to fibrates (Fig2c and SFig4a) consistent with the concept that fibrates
12 promote not only catabolic but also anabolic lipid pathways.
13
14
15
16
17
18

19 **P465L PPAR γ reduces serum VLDL levels in HFD fed mice.**

20
21 We next investigated whether changes in the lipoprotein lipid composition in P465L mice
22 mirrored their increased fat accumulation in liver as well as the identified blunted functional effect
23 of fibrates (Fig3ab). It has been previously reported that the hypolipidaemic effects of fibrates are
24 mostly due to enhanced catabolism of TG rich particles (increase lipoprotein lipase, LPL and
25 decrease Apolipoprotein CIII, apoCIII) and decreased in Apolipoprotein B (ApoB) and VLDL
26 production. Analysis of *VLDL* in chow fed conditions revealed that plasma levels of VLDL-TG in
27 P465L mice were greater than in WT mice. *A priori*, this increased levels of VLDL may has been
28 justified by the hyperinsulinemia of the P465L, leading to increased hepatic influx of FFA,
29 accumulation of TG and increased VLDL-TG secretion. However, what it was not expected was
30 that when fed HFD, the P465L mice showed a paradoxical decrease in VLDL-TG levels in plasma
31 compared to WT controls. Administration of WY14643 did not change VLDL-TG levels in mice
32 fed on chow of any genotype, but administration of WY14643 to WT mice fed HFD slightly
33 decreased VLDL-TG in line with the effects of fibrates in VLDL secretion (Fig3a). *ApocIII*
34 expression showed no genotype dependent differences and- as previously mentioned, the-P465L
35 mice showed a reduction in the plasma VLDL-TG levels, despite high fatty acid levels in serum. Of
36 potential pathogenic relevance fatty liver development, P465L livers had increased expression of
37 lipid droplet proteins such as Adipophilin/Perilipin2 (*adrp/plin2*) (Fig3c and SFig4a), Fat specific
38 protein 27/ Cell death inducing DFFA like effector C (*fsp27/cidec*) and s3-12/Perilipin 4 (*s3-*
39
40
41
42
43
44
45
46
47
48
49
50
51
52
53
54

1
2
3
4
5
6
7 *12/plin4*) as well as Fatty acid binding protein 4/ Adipocyte protein 2 (*fabp4/ap2*) (Fig3c and
8 SFig4a).
9

10 Gene expression analysis in chow fed conditions of genes involved in transport of lipids
11 confirmed that mRNA levels of hepatic (Fig3b) and adipose LPL (SFig3a), and of fatty acid
12 transporters *cd36* and *fatp1* in skeletal muscle (SFig3b) were decreased in P465L mice, in
13 agreement with the impaired peripheral metabolism of VLDL-TG in P465L mutants. Of note,
14 *apoIV* gene expression, which has been previously associated to hepatic steatosis and associated
15 with increased secretion of larger TG-enriched apoB-containing VLDL [31], was increased in
16 P465L livers, independently of the nutritional and pharmacological challenge. We also observed a
17 genotype dependent decrease in the levels of *apob* and minor differences in *mttp* (microsomal
18 triglyceride transfer protein).
19
20
21
22
23
24
25

26 We subsequently analysed the effect of P465L on HDL lipoproteins. Unlike in humans
27 where fibrates increase HDL-C levels and *apoa1* expression [32], fibrates have been reported not to
28 have any effect or even decrease the levels of HDL and *apoa1* expression in non-transgenic wild-
29 type mice [33, 34]. Surprisingly, in the P465L mice fed both chow and HFD, fibrates increased
30 HDL levels in comparison to WT mice. This finding indicates that P465L *Pparγ* mutation interferes
31 (directly or indirectly) with the normal response to fibrates on HDL metabolism.
32
33
34
35
36
37

38 Moreover, we also observed an increased *apoa2/apoa1* mRNA ratio in P465L mice (Fig3b).
39 Of note, increased levels of *apoa2* have been associated to increased pro-oxidative and pro-
40 inflammatory responses, alterations in the rate of HDL metabolism and increased atherogenic
41 risk [35]. Thus, this evidence indicates that the changes observed in P465L mutants result in a
42 deleterious effect on HDL metabolism.
43
44
45
46

47 WY14643 also increased cholesterol enriched IDL/LDL-C levels in both genotypes. A
48 similar effect has been previously reported for fenofibrate in mice fed high fat/high sucrose diets
49 [36] and in patients with severe dyslipidaemia [37]. We observed that in mice fed HFD, treatment
50 with WY14643 reduced the triglyceride enriched IDL/LDL-TG in WT but not in P465L mice
51
52
53
54

1
2
3
4
5
6
7 (Fig2B). This is in agreement with an decrease in the metabolisation of TG from the IDL/LDL
8 fraction, likely mediated by hepatic or peripheral lipases in P465L mice (where both levels of
9 hepatic lipase (HL) and Low density lipoprotein receptor (LDLR) are reduced) vs WT mice.
10

11
12 Globally considered, these findings indicate that the increase in triglyceride enriched VLDL-
13 TG plasma levels in chow fed P465L mice was the result of the increased flux of FFA into the liver
14 coupled with increased VLDL secretion and reduced peripheral/hepatic catabolism. Our data also
15 show a dietary related differential response characterised by increased VLDL levels linked to
16 increased flux of lipids into the liver under chow fed conditions in P465L mutant mice. This
17 contrasted with HFD phenotype defined by lower VLDL levels and increased hepatic steatosis.
18 These paradoxical responses suggest that the P465L mutant exhibits decreased metabolic flexibility
19 related to hepatic lipid handling, which becomes evident in the context of specific lipid related
20 nutritional and pharmacological challenges.
21
22

23 **Hepatic mitochondrial and peroxisomal FAO genes are downregulated in HFD fed P465L** 24 **mice.** 25 26

27
28 Fibrates promote a metabolic switch that favours the use of fatty acid as energetic substrates.
29 Fibrates are known to activate the pyruvate dehydrogenase kinases (PDK2 and PDK4), which
30 inactivate pyruvate dehydrogenase and enhance the utilization of serum fatty acids and triglycerides
31 [38]. The P465L livers showed reduced hepatic expression of *pdk4* in comparison to WT livers and
32 a blunted response to WY14643 in comparison to WT (Fig4a). Thus the P465L mutation prevents
33 the induction of fatty acid oxidation (FAO) by WY14643. The question was whether P465L PPAR γ
34 induced dysfunction in the mitochondrial and/or peroxisomal FAO programmes that could
35 contribute to the development of fatty liver and liver damage in P465L mice, as shown for other
36 models [39, 40].
37
38

39
40 P465L mutant mice showed reduced expression of mFAO and pFAO genes in chow fed
41 non-fibrate treated vs WT counterparts (Fig4b). These data may be interpreted as either P465L
42 PPAR γ preventing basal expression of genes regulated by PPAR α , and/or alternatively that
43
44
45
46
47
48

1
2
3
4
5
6
7 physiological expression PPAR γ itself may directly impair the expression of these genes. The latter
8 is unlikely given that the hepatic expression of PPAR γ under normal physiological conditions (i.e.
9 chow fed), is limited.
10

11
12 There is substantial literature showing a pro-oxidative role for PPAR α [41, 42]. In line with
13 this, WY14643 increased the expression of most of the genes associated to mFAO and pFAO
14 programmes in both genotypes. However, we identified a set of genes for mFAO and pFAO
15 programmes that failed to be upregulated in P465L livers in response to WY14643. Specifically
16 ATP-binding cassette subfamily D member 1 (*abcd1*), Phytanoyl-CoA 2 Hydroxylase (*phyh*)
17 ,Isocitrate Dehydrogenase (*idh*), Enoyl-CoA Hydratase 1 (*ech1*), 2,4-Dienoyl-CoA Reductase 2
18 (*decr2*), failed to be induced by fibrates in P465L liver, providing evidence of selective resistance to
19 the transcriptional response to fibrates (Fig4b). We also identified genes that responded differently
20 in P465L vs WT livers when fed chow or HFD diets (Long chain Acyl-CoA Dehydrogenase, *lcad*;
21 Medium chain Acyl-CoA Dehydrogenase *mcd*; Very Long chain Acyl-CoA synthase *vlcas*; Alpha
22 methyl-acyl-CoA Racemase *amacr*; Malonyl-CoA Decarboxylase, *mylcd*). This suggested an
23 interaction effect of the genotype with both, fibrate treatment and dietary challenges.
24
25

26
27 When assessing the expression FAO genes in mice fasted overnight we did not observe strong
28 changes associated to P465L mutation apart from *abcd1*, *scp2* (GxF interactive effect) (SFig4).
29

30
31 Finally, we also evaluated the expression of other transcription factors apart from *ppar α* and *ppar γ* ,
32 involved in the transcriptional activation of multiple lipid related genes (Fig4c) and whose
33 expression could also be dysregulated by the activation of *ppar α* (fibrates) and the P465L mutation.
34
35 In this regard, fibrates and P465L affected the expression of *srebp1*, *hnf4*, *rxr* (Fig4c). Interestingly,
36 the expression of *ppar γ* at gene and protein level (Fig4c and SFig4a) was upregulated in P465L
37 mutant livers, increasing the pool of the WT and also the mutant P465L- *ppar γ* and thus competing
38 with *ppar α* in response to fibrates when both transcription factors are upregulated (Fig4c and
39 SFig4a).
40
41
42
43
44
45
46
47
48
49
50
51
52
53
54
55
56
57
58
59
60

P465L PPAR γ interferes with the transrepression capacity of PPAR α .

Fibrates also exert anti-fibrotic and anti-inflammatory effects through transrepressive mechanisms [43]. We observed that in HFD fed WT mice, administration of WY14643 reduces the expression of target genes such as *serum amyloid A (saa1 and saa2)* and *fibrinogen* (Fig5). Interestingly, this effect was not observed in P465L mice suggesting that this mutation also prevented the transrepression activity of PPAR α .

Discussion

This work follows previous research from us and others on the P465L mouse, a humanized model for the dominant negative mutant P467L PPAR γ that resembles the phenotype observed in patients and characterised by a partial lipodystrophy, insulin resistance, hypertension and fatty liver.

Here, we provide evidence that the fatty liver observed in the P465L PPAR γ knock-in mouse involves a selective impairment in the transcriptional activation of PPAR α . This is supported by *in vivo* data showing that P465L mice developed fatty liver on a HFD and were resistant to treatment with WY14643, a fibrate that acts as a PPAR α activator, determining a phenotype highly reminiscent of the resistance to fibrates previously observed in PPAR α KO mice [44]. We have shown that in response to WY14643, the size of the fat depots is decreased in WT mice whereas P465L adipose tissues remain unaffected. Similarly, whereas WY14643 treated HFD WT mice showed a reduction in hepatic TG content, the P465L did not and additionally, we observed exacerbated hepatic accumulation of TG during the fed/fasting transition in P465L mice fed chow or HFD. These responses are supportive of a partial resistance to the effects of PPAR α activation in P465L mice.

We have learned that the PPAR γ P465L mutant interferes with the lipoprotein profile and its regulation by fibrates. We observed a shift in the lipoprotein fingerprint between chow and HFD fed P465L mice. When fed a chow diet, P465L mice had increased levels of VLDL compared to WT

1
2
3
4
5
6
7 mice, an observation consistent with an increased flux of fatty acids originated in the leak from a
8 dysfunctional adipose tissue and associated hyperinsulinemia. However, when fed HFD for 28d, the
9 pattern of VLDLs was reversed, showing decreased levels of VLDL coupled with increased
10 expression of hepatic lipid droplet proteins in the P465L PPAR γ mutant livers. Whether this
11 increase in lipid droplet protein expression in mutant livers is directly mediated by a disordered
12 transcriptional programme of PPAR γ or merely a secondary perturbation is unclear. It is well
13 known that PPAR γ and PPAR α are both transcriptional regulators of *adrp/plin2* and *fsp27/cidec*
14 [45] and that the overexpression of *fsp27/cidec* and *adrp/plin2* prevents the access of lipases to the
15 core of the lipid droplet thus impairing the hydrolysis of TG [46, 47]. Thus, the increased
16 expression of lipid droplet proteins may be a relevant pathogenic factor for hepatic steatosis [48]
17 contributing to the accumulation of lipids in the in P465L mice. Of note, *fsp27/cidec* expression is
18 further increased in P465L livers with fibrates, which may contribute to the increase in hepatic TG
19 levels in HFD fed P465L in comparison to WT mice. This apparent paradox of PPAR α
20 simultaneously promoting the expression of lipid droplet proteins that limit the mobilization of lipid
21 from the liver, together with PPAR α promoting lipid oxidation, suggest the relevance of PPAR α for
22 the activation of genetic programmes aimed to reduce the accumulation of potential toxic lipid
23 species by a double strategy that involves either diverting lipids either to a safe storage and/or
24 metabolising them. This duality of functions may explain the apparent controversial disparate
25 results observed with the use of fibrates to treat fatty liver in several rodent models [49, 50],
26 particularly when one of these two programmes may prevail over the other.
27
28
29
30
31
32
33
34
35
36
37
38
39
40
41
42
43

44 It is assumed that the association between lipodystrophy and NAFLD is direct consequence
45 of the failure of the adipose tissue to expand and the consequent spillage of excessive lipids into the
46 liver. Here, we provide evidence that the fatty liver of the P465L lipodystrophic mice exhibit not
47 only quantitative but also qualitative changes (increased MUFA/PUFA ratio) in the accumulate
48 lipids. These data are thus consistent with changes in hepatic lipid biosynthetic pathways
49 characteristic of “classical models” of NAFLD, and indicate that these qualitative changes in the
50
51
52
53
54

1
2
3
4
5
6
7 fatty acid pool of P465L livers may reflect a common pathogenic signature of NAFLD, rather than
8 a specific fingerprint driven by the presence of the PPAR γ mutation.
9

10 Our expression profiling revealed selective impairment of PPAR α preferentially regulated
11 genes in P465L mice on a chow diet, treated only with vehicle. This indicates that even when
12 PPAR α ligands are present at low physiological levels, the presence of the P465L mutation is
13 enough to dysregulate the expression of those PPAR α genes at a transcriptional level. The P465L
14 mice fed a chow diet showed also impaired expression of genes controlling mFAO and pFAO -
15 well-known targets of PPAR α in mice. These effects were partially masked after treatment with
16 WY14643 and/or HFD. Additionally, we also identified genes in the P465L livers that remained
17 pathologically unresponsive to treatment with fibrates in comparison to WT providing compelling
18 evidence of resistance to the ligand-dependent activation of PPAR α when P465L PPAR γ is present.
19 Interestingly, genotype driven differences were reduced when mice were fasted overnight (GxF
20 interactive effect), indicating that the effect of the P465L mutation on PPAR α function may only
21 become pathophysiologically relevant at basal levels, when the expression/activity of PPAR α is
22 below a particular threshold or alternatively that it may become overcome by the hormonal
23 adaptation taking place in response to starvation.
24
25
26
27
28
29
30
31
32
33
34
35
36

37 Despite the fact that our experimental model of treatment with HFD/WY14643 was not
38 specifically designed to induce severe liver damage, we found that the expression of genes involved
39 in fibrosis- and known to be downregulated by PPAR α activation- were altered in P465L livers,
40 suggesting that transrepression activity of PPAR α was also impaired by the presence of the P465L
41 PPAR γ mutant.
42
43
44
45

46 Globally considered, our data indicate that the pathogenesis of the fatty liver observed in
47 P465L mice is more complex than simply the result of the failure of the adipose, and that it involves
48 the combination of several pathogenic factors at hepatic level including uncoupling the lipid storage
49
50
51
52
53
54

1
2
3
4
5
6
7 in lipid droplets from the assembly, transport and secretion of VLDL, associated to impaired hepatic
8
9
10
11
12
13
14
15
16
17
18
19
20
21
22
23
24
25
26
27
28
29
30
31
32
33
34
35
36
37
38
39
40
41
42
43
44
45
46
47
48
49
50
51
52
53
54
55
56
57
58
59
60

in lipid droplets from the assembly, transport and secretion of VLDL, associated to impaired hepatic
FAO in a pathological context where peripheral uptake of lipids is likely to be compromised.

In summary, we have shown that P465L mice develop hepatic steatosis associated to increased lipid trapping and impaired VLDL secretion with HFD, resulting in qualitative changes in the hepatic fatty acids that recapitulates the fingerprint of common NAFLD models. We also provide biochemical data, hepatic lipid content and evidence of impaired expression of a number of well-established PPAR α target genes in P465L livers that supports the conclusion that P465L confers partial resistance to the hypolipidemic action of fibrates. Moreover, our results also show that the fatty liver phenotype observed in P465L mutant mice is not only the consequence of dysfunctional adipose tissue, but also involves defective liver metabolism. Despite the current lack of trials addressing the efficacy of fibrates in patients with partial lipodystrophy, our results raise concerns regarding the potential value of fibrates for the management of hypertriglyceridemia/NAFLD in carriers of the dominant negative P467L-PPAR γ mutation. Whether our findings are transferable to the overall FPLD3 spectrum of diseases is currently unknown. However, there are reports of FPLD3 patients, characterised by recurrent hypertriglyceridemia despite treatment with fibrates [20-23]. Finally, our data also indicate that the specific repertoire of PPARs present under specific metabolic conditions is important as it may modulate the fine balance between transcription factors with metabolically opposed functions.

Funding

This work was funded by Wellcome Trust, MRC MDU (MC_UU_12012/2), FP7-MITIN (Integration of the System Models of Mitochondrial Function and Insulin Signalling and its Application in the Study of Complex Diseases (Grant Agreement 223450) and H2020 EPoS Elucidating Pathways of Steatohepatitis. (Grant Agreement 634413). Disease Model Core, Biochemistry Assay Lab and the Histology Core are funded by [MRC_MC_UU_12012/5] and Wellcome Trust Strategic Award [100574/Z/12/Z].

1
2
3
4
5
6
7 **Author Contributions.** SRC and SC conceived the original hypothesis, designed and performed
8 experiments in vivo/ex vivo and wrote the manuscript. GBC performed the fatty acid composition
9 analysis, discussed and edited the manuscript. XP performed the lipoprotein profiling, discussed
10 and edited the manuscript, RA, JR, MC, RD and MB contributed to ex vivo profiling, discussed and
11 edited the manuscript. SG conceived the original hypothesis, designed experiments and wrote the
12 manuscript. AVP conceived the original hypothesis, designed experiments and wrote the
13 manuscript. AVP is the guarantor of this work. All authors approved its publication.
14
15
16

17
18 **Conflict of interest.** The authors declare that they have no conflict of interest.
19
20
21
22
23
24
25
26
27
28
29
30
31
32
33
34
35
36
37
38
39
40
41
42
43
44
45
46
47
48
49
50
51
52
53
54
55
56
57
58
59
60

FIGURE LEGENDS

FIGURE1. (a) Blood biochemistry and Body composition (b) from P465L ppar γ mutant mice vs. WT mice fed chow or HFD, with or without WY14643 (ip:25mg/kg). Graphs represent the average of 7-8 mice per group \pm SEM analysed by ANOVA ($p < 0.05$). Different colour circles denote genotype effect (blue), treatment (red), diet (green), interactive effect genotype x treatment (black), genotype x diet (white), diet x treatment (grey) and genotype x treatment x diet (orange).

FIGURE2. (a) Oil Red O -stained sections (10 \times) and triglyceride composition of liver from P465L ppar γ mutant mice vs. WT mice fed chow or HFD, with or without WY14643 (ip:25mg/kg). Graphs represent the average of 7-8 mice per group \pm SEM. (b) Fatty acid composition in molar percentage of hepatic fatty acids from P465L ppar γ mutant mice vs. WT mice fed chow or HFD, with or without WY14643 (ip:25mg/kg). (c) Hepatic gene expression of candidate genes relevant in *de novo* lipogenesis and PUFA biosynthesis and analysed by ANOVA ($p < 0.05$). Different colour circles denote Genotype effect (blue), treatment (red), diet (green), interactive effect genotype x treatment (black), genotype x diet (white), diet x treatment (grey) and genotype x treatment x diet (orange).

FIGURE3. (a) Lipoprotein cholesterol and TG distribution were determined in plasma from non-fasted P465L ppar γ mutant mice vs. WT mice fed chow or HFD, with or without WY14643 (ip:25mg/kg). Approximate elution volumes for particles in the size ranges of VLDL, LDL, and HDL are indicated (b) Hepatic gene expression of candidate genes relevant in lipoprotein metabolism and (c) lipid droplet proteins is shown as log₂ conversions of average gene expression data relative to controls (log₂ 100 = 6.6). Magnitude > 6.6 and < 6.6 denotes up- and downregulation, respectively, compared with WT, chow fed controls and analysed by ANOVA ($p < 0.05$). Different colour circles denote Genotype effect (blue), treatment (red), diet (green), interactive effect genotype x treatment (black), genotype x diet (white), diet x treatment (grey) and genotype x treatment x diet (orange).

FIGURE4. (a) Hepatic gene expression of candidate genes relevant in (a) glucose metabolism (b) fatty acid uptake and mitochondrial/peroxisomal fatty acid oxidation programmes and (c) nuclear transcription factors is shown as log₂ conversions of average gene expression data relative to controls (log₂ 100 = 6.6). Magnitude > 6.6 and < 6.6 denotes up- and downregulation, respectively, compared with WT, chow fed controls and analysed by ANOVA ($p < 0.05$). Different colour circles denote Genotype effect (blue), treatment (red), diet (green), interactive effect genotype x treatment (black), genotype x diet (white), diet x treatment (grey) and genotype x treatment x diet (orange).

FIGURE5. (a) Hepatic gene expression of candidate genes relevant in inflammation and fibrosis is shown as log₂ conversions of average gene expression data relative to controls (log₂ 100 = 6.6). Magnitude > 6.6 and < 6.6 denotes up- and downregulation, respectively, compared with WT, chow fed controls and analysed by ANOVA ($p < 0.05$). Different colour circles denote Genotype effect (blue), treatment (red), diet (green), interactive effect genotype x treatment (black), genotype x diet (white), diet x treatment (grey) and genotype x treatment x diet (orange).

REFERENCES

- [1] Evans RM, Barish GD, Wang YX. PPARs and the complex journey to obesity. *Nat Med*. 2004; **10**: 355-361
- [2] Rodriguez-Cuenca S, Carobbio S, Velagapudi VR, *et al*. Peroxisome proliferator-activated receptor gamma-dependent regulation of lipolytic nodes and metabolic flexibility. *Mol Cell Biol*. 2012; **32**: 1555-1565
- [3] Majithia AR, Tsuda B, Agostini M, *et al*. Prospective functional classification of all possible missense variants in PPARG. *Nat Genet*. 2016; **48**: 1570-1575
- [4] Garg A. Acquired and inherited lipodystrophies. *N Engl J Med*. 2004; **350**: 1220-1234
- [5] Gray SL, Nora ED, Grosse J, *et al*. Leptin deficiency unmasks the deleterious effects of impaired peroxisome proliferator-activated receptor gamma function (P465L PPARgamma) in mice. *Diabetes*. 2006; **55**: 2669-2677
- [6] Kis A, Murdoch C, Zhang M, *et al*. Defective peroxisomal proliferators activated receptor gamma activity due to dominant-negative mutation synergizes with hypertension to accelerate cardiac fibrosis in mice. *Eur J Heart Fail*. 2009; **11**: 533-541
- [7] Pendse AA, Johnson LA, Tsai YS, Maeda N. Pparg-P465L mutation worsens hyperglycemia in Ins2-Akita female mice via adipose-specific insulin resistance and storage dysfunction. *Diabetes*. 2010; **59**: 2890-2897
- [8] Vidal-Puig A, Jimenez-Linan M, Lowell BB, *et al*. Regulation of PPAR gamma gene expression by nutrition and obesity in rodents. *J Clin Invest*. 1996; **97**: 2553-2561
- [9] Oosterveer MH, Grefhorst A, van Dijk TH, *et al*. Fenofibrate simultaneously induces hepatic fatty acid oxidation, synthesis, and elongation in mice. *J Biol Chem*. 2009; **284**: 34036-34044
- [10] Issemann I, Green S. Activation of a member of the steroid hormone receptor superfamily by peroxisome proliferators. *Nature*. 1990; **347**: 645-650
- [11] Hashimoto T, Cook WS, Qi C, Yeldandi AV, Reddy JK, Rao MS. Defect in peroxisome proliferator-activated receptor alpha-inducible fatty acid oxidation determines the severity of hepatic steatosis in response to fasting. *J Biol Chem*. 2000; **275**: 28918-28928
- [12] Guerre-Millo M, Rouault C, Poulain P, *et al*. PPAR-alpha-null mice are protected from high-fat diet-induced insulin resistance. *Diabetes*. 2001; **50**: 2809-2814
- [13] Chou CJ, Haluzik M, Gregory C, *et al*. WY14,643, a peroxisome proliferator-activated receptor alpha (PPARalpha) agonist, improves hepatic and muscle steatosis and reverses insulin resistance in lipoatrophic A-ZIP/F-1 mice. *J Biol Chem*. 2002; **277**: 24484-24489
- [14] Semple RK, Meirhaeghe A, Vidal-Puig AJ, *et al*. A dominant negative human peroxisome proliferator-activated receptor (PPAR){alpha} is a constitutive transcriptional corepressor and inhibits signaling through all PPAR isoforms. *Endocrinology*. 2005; **146**: 1871-1882
- [15] Gervois P, Torra IP, Chinetti G, *et al*. A truncated human peroxisome proliferator-activated receptor alpha splice variant with dominant negative activity. *Mol Endocrinol*. 1999; **13**: 1535-1549
- [16] Savage DB, Tan GD, Acerini CL, *et al*. Human metabolic syndrome resulting from dominant-negative mutations in the nuclear receptor peroxisome proliferator-activated receptor-gamma. *Diabetes*. 2003; **52**: 910-917
- [17] Agostini M, Gurnell M, Savage DB, *et al*. Tyrosine agonists reverse the molecular defects associated with dominant-negative mutations in human peroxisome proliferator-activated receptor gamma. *Endocrinology*. 2004; **145**: 1527-1538
- [18] Barroso I, Gurnell M, Crowley VE, *et al*. Dominant negative mutations in human PPARgamma associated with severe insulin resistance, diabetes mellitus and hypertension. *Nature*. 1999; **402**: 880-883
- [19] Leff T, Mathews ST, Camp HS. Review: peroxisome proliferator-activated receptor-gamma and its role in the development and treatment of diabetes. *Exp Diabetes Res*. 2004; **5**: 99-109

- 1
2
3
4
5
6
7 [20] Li G, Leff T. Altered promoter recycling rates contribute to dominant-negative activity of
8 human peroxisome proliferator-activated receptor-gamma mutations associated with diabetes. *Mol*
9 *Endocrinol.* 2007; **21**: 857-864
- 10 [21] Hegele RA. Lessons from human mutations in PPARgamma. *Int J Obes (Lond).* 2005; **29**
11 **Suppl 1**: S31-35
- 12 [22] Folch J, Lees M, Sloane Stanley GH. A simple method for the isolation and purification of
13 total lipides from animal tissues. *J Biol Chem.* 1957; **226**: 497-509
- 14 [23] Pons A, Roca P, Aguilo C, Garcia FJ, Alemany M, Palou A. A method for the simultaneous
15 determination of total carbohydrate and glycerol in biological samples with the anthrone reagent. *J*
16 *Biochem Biophys Methods.* 1981; **4**: 227-231
- 17 [24] Castagnet PI, Golovko MY, Barcelo-Coblijn GC, Nussbaum RL, Murphy EJ. Fatty acid
18 incorporation is decreased in astrocytes cultured from alpha-synuclein gene-ablated mice. *J*
19 *Neurochem.* 2005; **94**: 839-849
- 20 [25] Hara A, Radin NS. Lipid extraction of tissues with a low-toxicity solvent. *Anal Biochem.*
21 1978; **90**: 420-426
- 22 [26] Brockerhoff H. Determination of the positional distribution of fatty acids in glycerolipids.
23 *Methods Enzymol.* 1975; **35**: 315-325
- 24 [27] Vandesompele J, De Preter K, Pattyn F, *et al.* Accurate normalization of real-time
25 quantitative RT-PCR data by geometric averaging of multiple internal control genes. *Genome Biol.*
26 2002; **3**: RESEARCH0034
- 27 [28] Lu Y, Boekschoten MV, Wopereis S, Muller M, Kersten S. Comparative transcriptomic and
28 metabolomic analysis of fenofibrate and fish oil treatments in mice. *Physiol Genomics.* 2011; **43**:
29 1307-1318
- 30 [29] Ferreira AV, Parreira GG, Green A, Botion LM. Effects of fenofibrate on lipid metabolism
31 in adipose tissue of rats. *Metabolism.* 2006; **55**: 731-735
- 32 [30] Blanchard H, Legrand P, Pedrono F. Fatty Acid Desaturase 3 (Fads3) is a singular member
33 of the Fads cluster. *Biochimie.* 2011; **93**: 87-90
- 34 [31] VerHague MA, Cheng D, Weinberg RB, Shelness GS. Apolipoprotein A-IV expression in
35 mouse liver enhances triglyceride secretion and reduces hepatic lipid content by promoting very
36 low density lipoprotein particle expansion. *Arterioscler Thromb Vasc Biol.* 2013; **33**: 2501-2508
- 37 [32] Tsunoda F, Asztalos IB, Horvath KV, Steiner G, Schaefer EJ, Asztalos BF. Fenofibrate,
38 HDL, and cardiovascular disease in Type-2 diabetes: The DAIS trial. *Atherosclerosis.* 2016; **247**:
39 35-39
- 40 [33] Berthou L, Duverger N, Emmanuel F, *et al.* Opposite regulation of human versus mouse
41 apolipoprotein A-I by fibrates in human apolipoprotein A-I transgenic mice. *J Clin Invest.* 1996; **97**:
42 2408-2416
- 43 [34] Vu-Dac N, Chopin-Delannoy S, Gervois P, *et al.* The nuclear receptors peroxisome
44 proliferator-activated receptor alpha and Rev-erbalpha mediate the species-specific regulation of
45 apolipoprotein A-I expression by fibrates. *J Biol Chem.* 1998; **273**: 25713-25720
- 46 [35] Castellani LW, Lusis AJ. ApoA-II versus ApoA-I: two for one is not always a good deal.
47 *Arterioscler Thromb Vasc Biol.* 2001; **21**: 1870-1872
- 48 [36] Fernandes-Santos C, Carneiro RE, de Souza Mendonca L, Aguila MB, Mandarim-de-
49 Lacerda CA. Pan-PPAR agonist beneficial effects in overweight mice fed a high-fat high-sucrose
50 diet. *Nutrition.* 2009; **25**: 818-827
- 51 [37] Davignon J, Roederer G, Montigny M, *et al.* Comparative efficacy and safety of pravastatin,
52 nicotinic acid and the two combined in patients with hypercholesterolemia. *Am J Cardiol.* 1994; **73**:
53 339-345
- 54 [38] Motojima K. A metabolic switching hypothesis for the first step in the hypolipidemic effects
55 of fibrates. *Biol Pharm Bull.* 2002; **25**: 1509-1511
- 56 [39] Cherkaoui-Malki M, Surapureddi S, El-Hajj HI, Vamecq J, Andreoletti P. Hepatic steatosis
57 and peroxisomal fatty acid beta-oxidation. *Curr Drug Metab.* 2012; **13**: 1412-1421

- 1
2
3
4
5
6
7 [40] Mantena SK, King AL, Andringa KK, Eccleston HB, Bailey SM. Mitochondrial dysfunction
8 and oxidative stress in the pathogenesis of alcohol- and obesity-induced fatty liver diseases. *Free*
9 *Radic Biol Med.* 2008; **44**: 1259-1272
- 10 [41] Chamouton J, Latruffe N. PPARalpha/HNF4alpha interplay on diversified responsive
11 elements. Relevance in the regulation of liver peroxisomal fatty acid catabolism. *Curr Drug Metab.*
12 2012; **13**: 1436-1453
- 13 [42] Rodriguez C, Cabrero A, Roglans N, *et al.* Differential induction of stearoyl-CoA desaturase
14 and acyl-CoA oxidase genes by fibrates in HepG2 cells. *Biochem Pharmacol.* 2001; **61**: 357-364
- 15 [43] Pawlak M, Bauge E, Bourguet W, *et al.* The transrepressive activity of peroxisome
16 proliferator-activated receptor alpha is necessary and sufficient to prevent liver fibrosis in mice.
17 *Hepatology.* 2014; **60**: 1593-1606
- 18 [44] Montagner A, Polizzi A, Fouche E, *et al.* Liver PPARalpha is crucial for whole-body fatty
19 acid homeostasis and is protective against NAFLD. *Gut.* 2016; **65**: 1202-1214
- 20 [45] de la Rosa Rodriguez MA, Kersten S. Regulation of lipid droplet-associated proteins by
21 peroxisome proliferator-activated receptors. *Biochim Biophys Acta.* 2017; **1862**: 1212-1220
- 22 [46] Langhi C, Baldan A. CIDEC/FSP27 is regulated by peroxisome proliferator-activated
23 receptor alpha and plays a critical role in fasting- and diet-induced hepatosteatosis. *Hepatology.*
24 2015; **61**: 1227-1238
- 25 [47] Rajamoorthi A, Arias N, Basta J, Lee RG, Baldan A. Amelioration of diet-induced
26 steatohepatitis in mice following combined therapy with ASO-Fsp27 and fenofibrate. *J Lipid Res.*
27 2017:
- 28 [48] Fujii H, Ikura Y, Arimoto J, *et al.* Expression of perilipin and adipophilin in nonalcoholic
29 fatty liver disease; relevance to oxidative injury and hepatocyte ballooning. *J Atheroscler Thromb.*
30 2009; **16**: 893-901
- 31 [49] Edvardsson U, Ljungberg A, Linden D, *et al.* PPARalpha activation increases triglyceride
32 mass and adipose differentiation-related protein in hepatocytes. *J Lipid Res.* 2006; **47**: 329-340
- 33 [50] Shiri-Sverdlov R, Wouters K, van Gorp PJ, *et al.* Early diet-induced non-alcoholic
34 steatohepatitis in APOE2 knock-in mice and its prevention by fibrates. *J Hepatol.* 2006; **44**: 732-
35 741
- 36
37
38
39
40
41
42
43
44
45
46
47
48
49
50
51
52
53
54
55
56
57
58
59
60

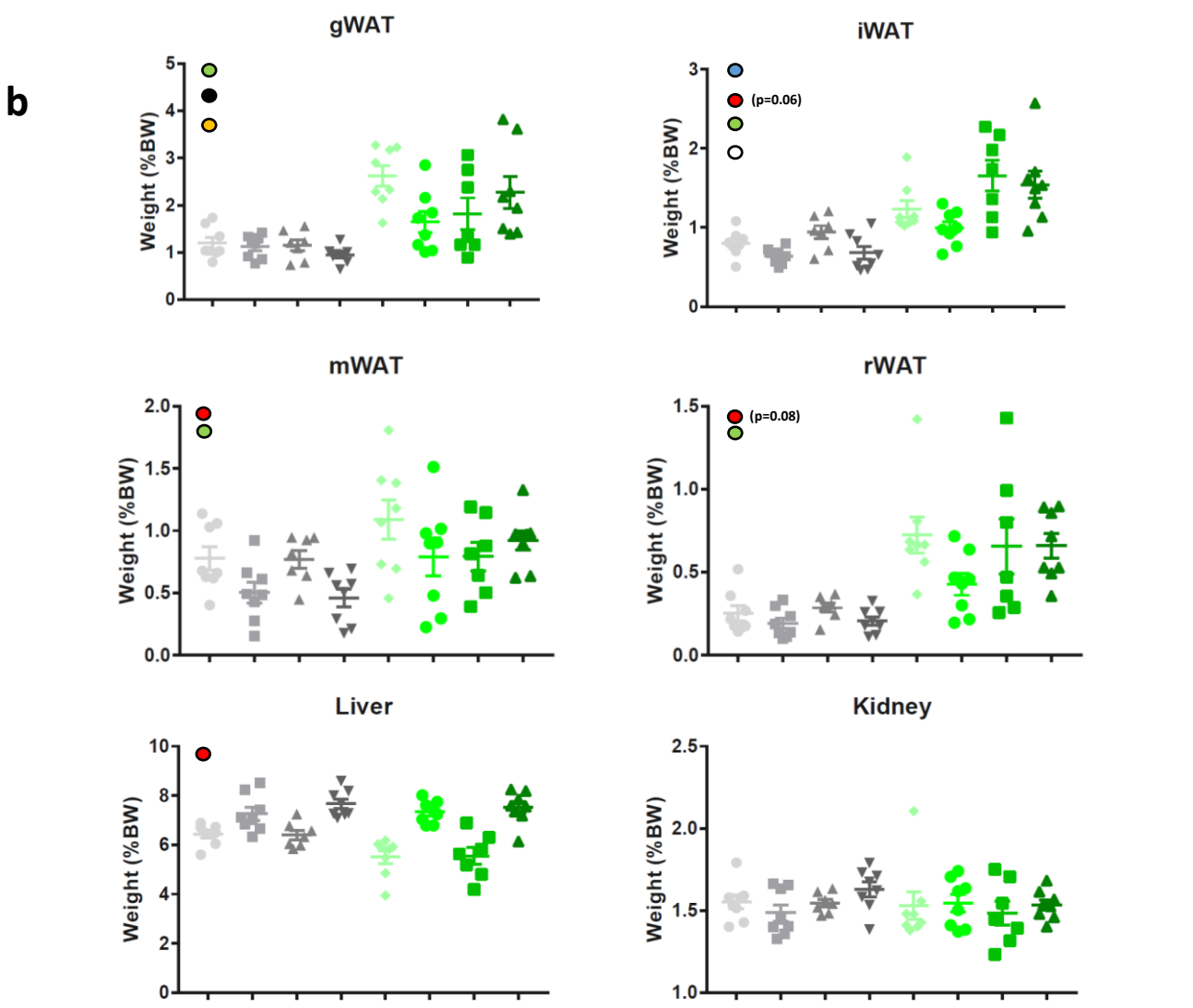
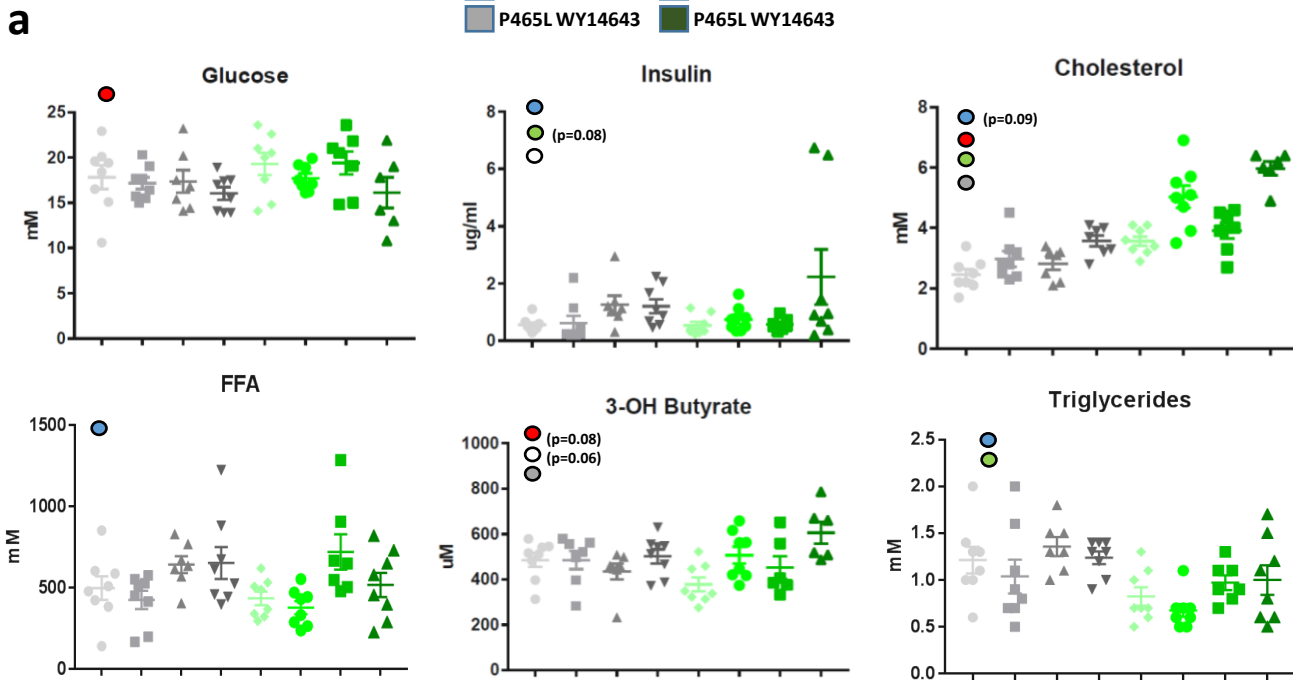
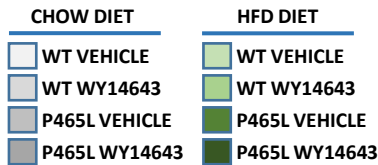
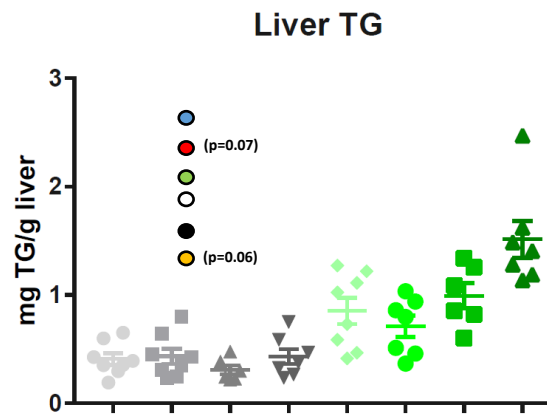
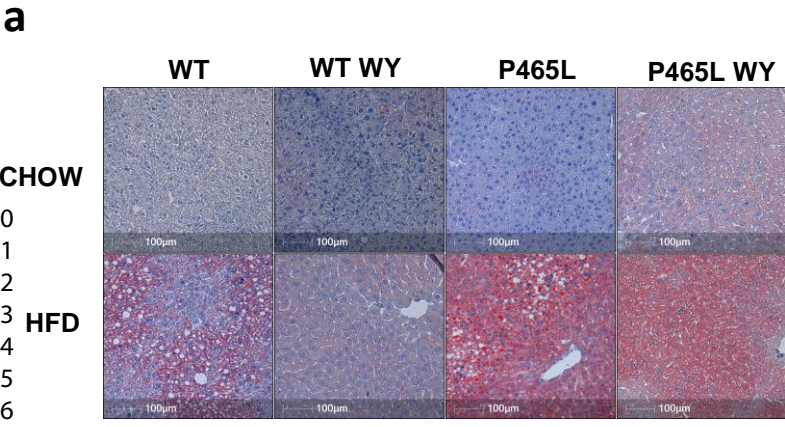
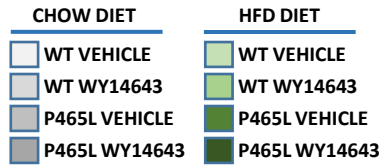
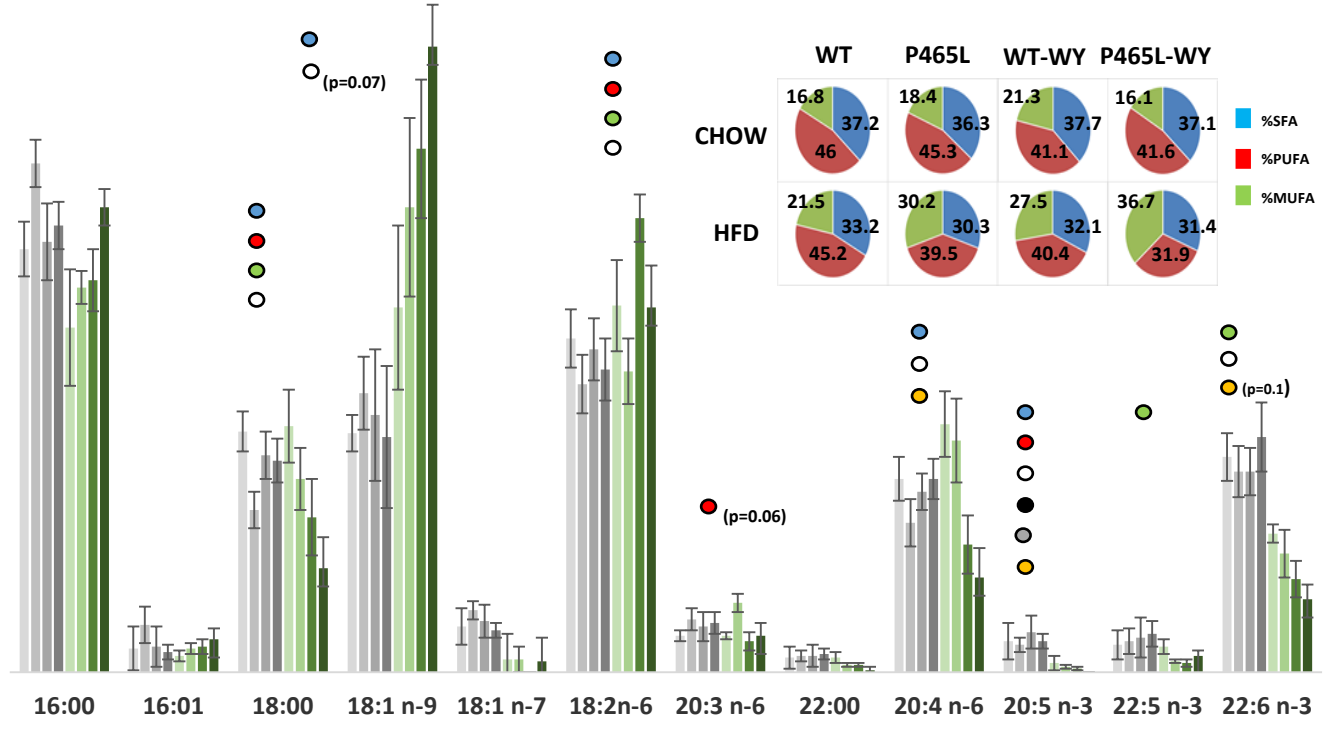


FIG 1

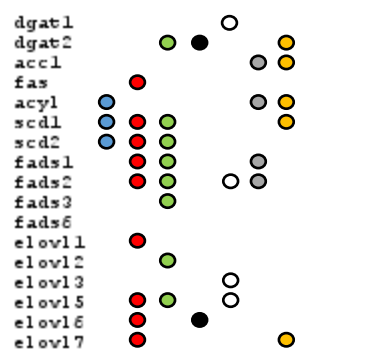
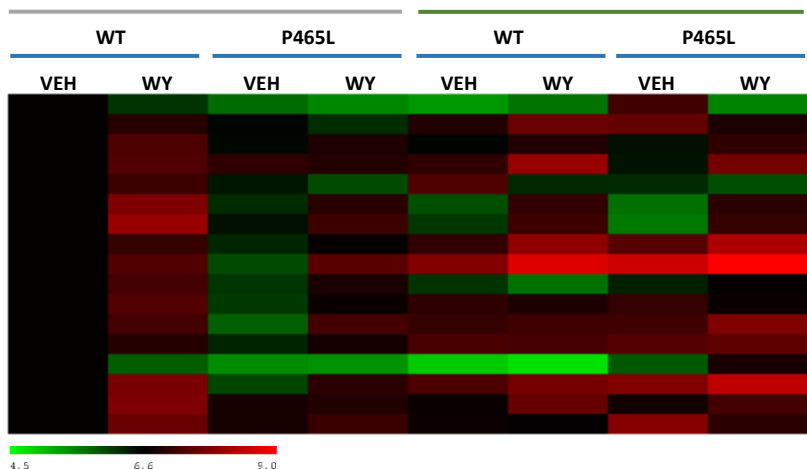
1
2
3
4
5
6
7
8
9
10
11
12
13
14
15
16
17
18
19
20
21
22
23
24
25
26
27
28
29
30
31
32
33
34
35
36
37
38
39
40
41
42
43
44
45
46
47
48
49
50
51
52
53
54
55
56
57
58
59
60



HEPATIC FATTY ACID COMPOSITION (%)



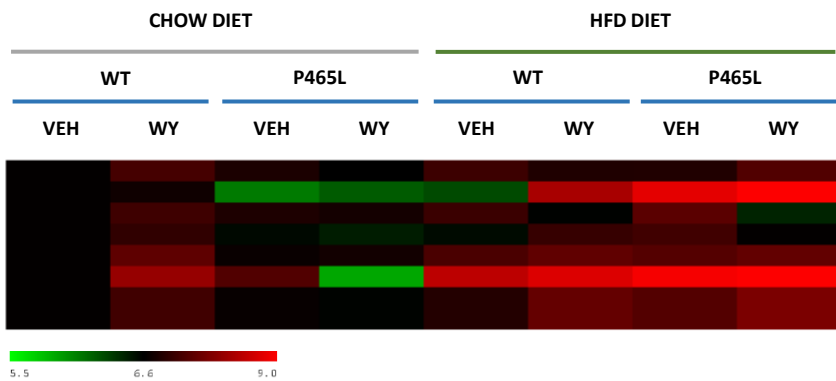
CHOW DIET HFD DIET



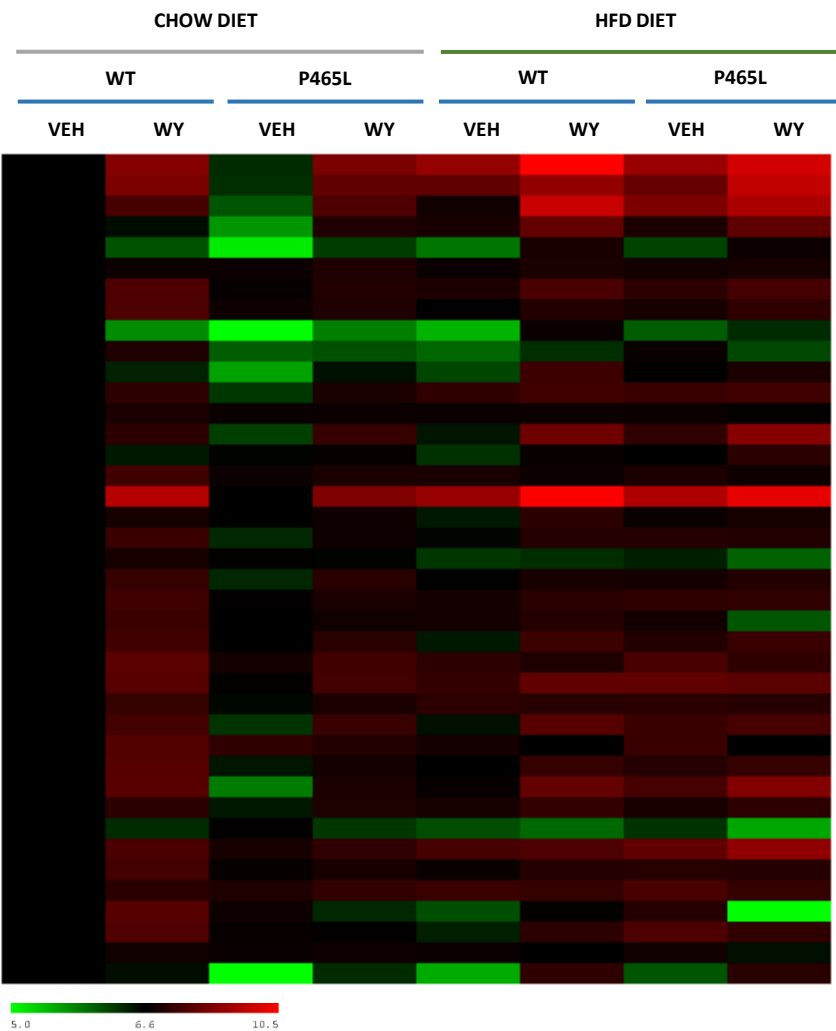
● G ● T ● D ● GxT ● GxD ● TxD ● GxTxD

FIG 2

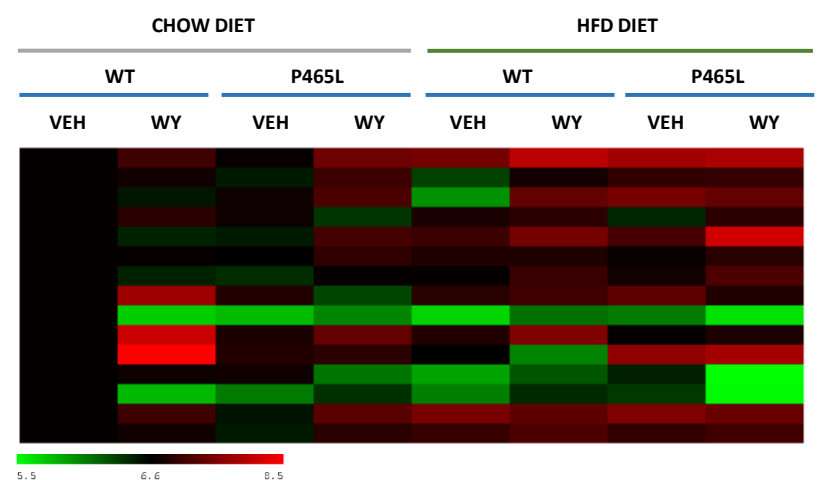
a



b



c



● G ● T ● D ● GxT ○ GxD ○ TxD ● GxTxD

FIG 4

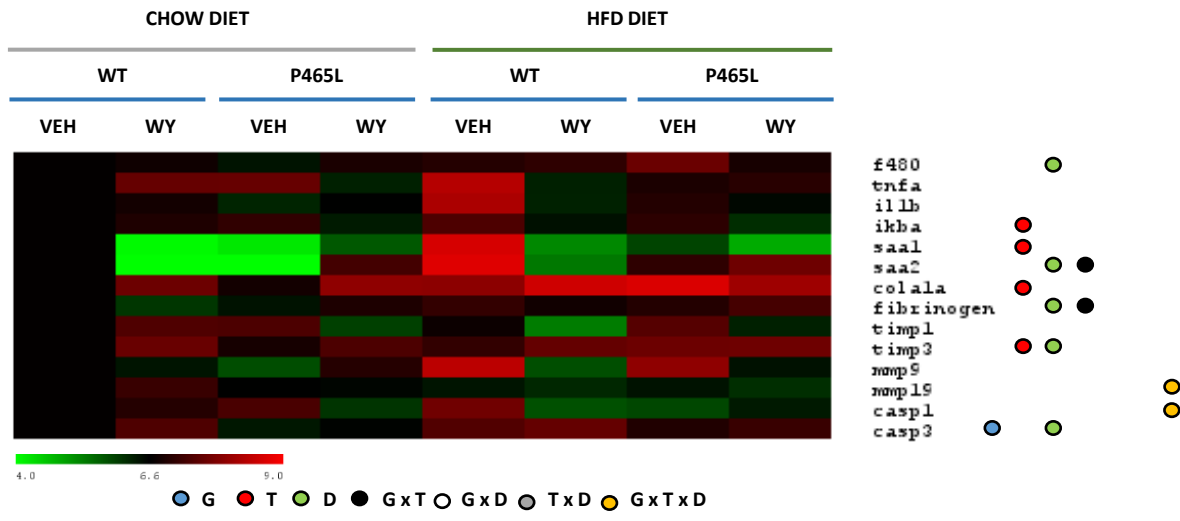
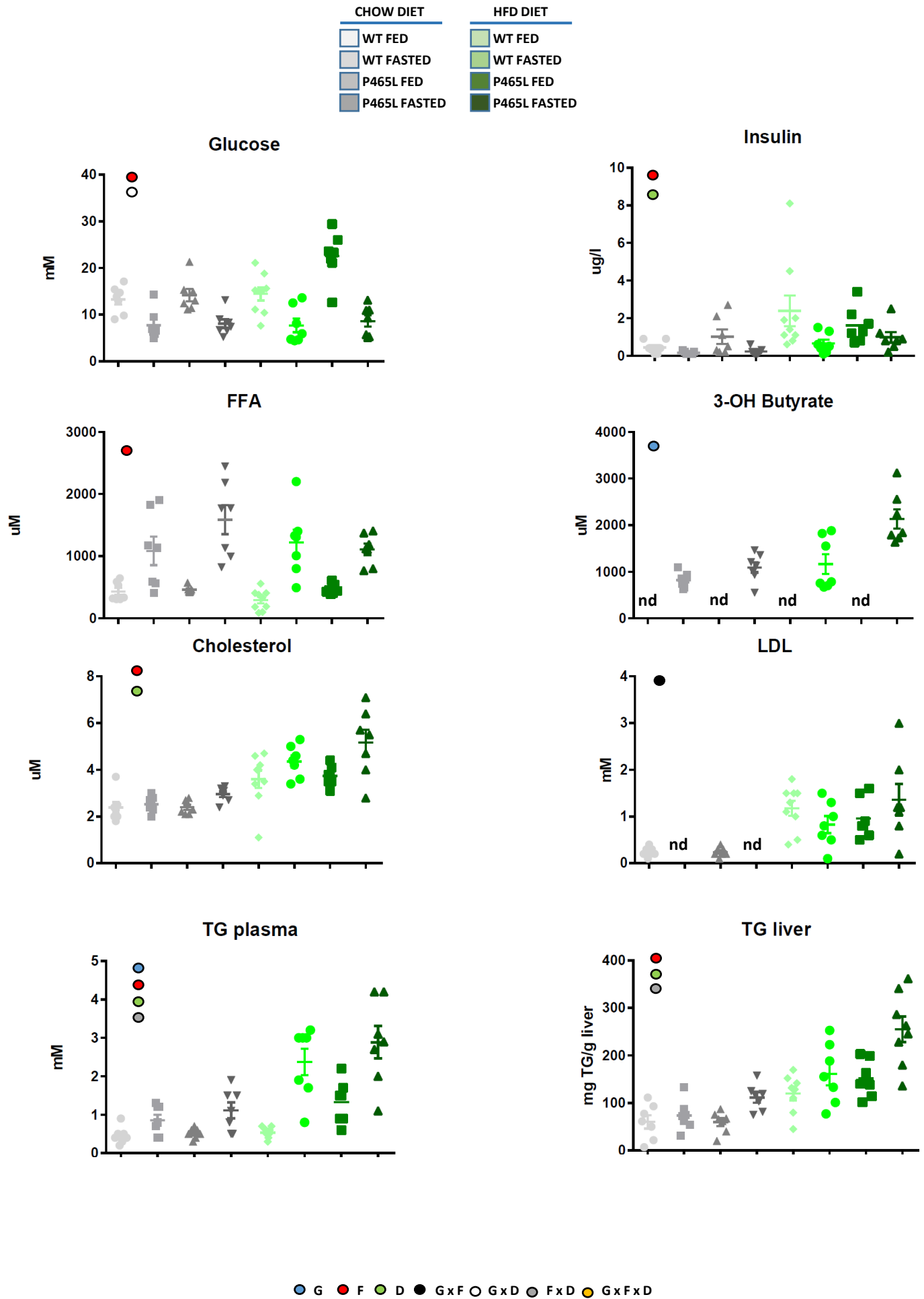
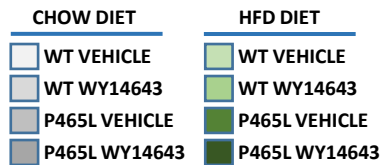


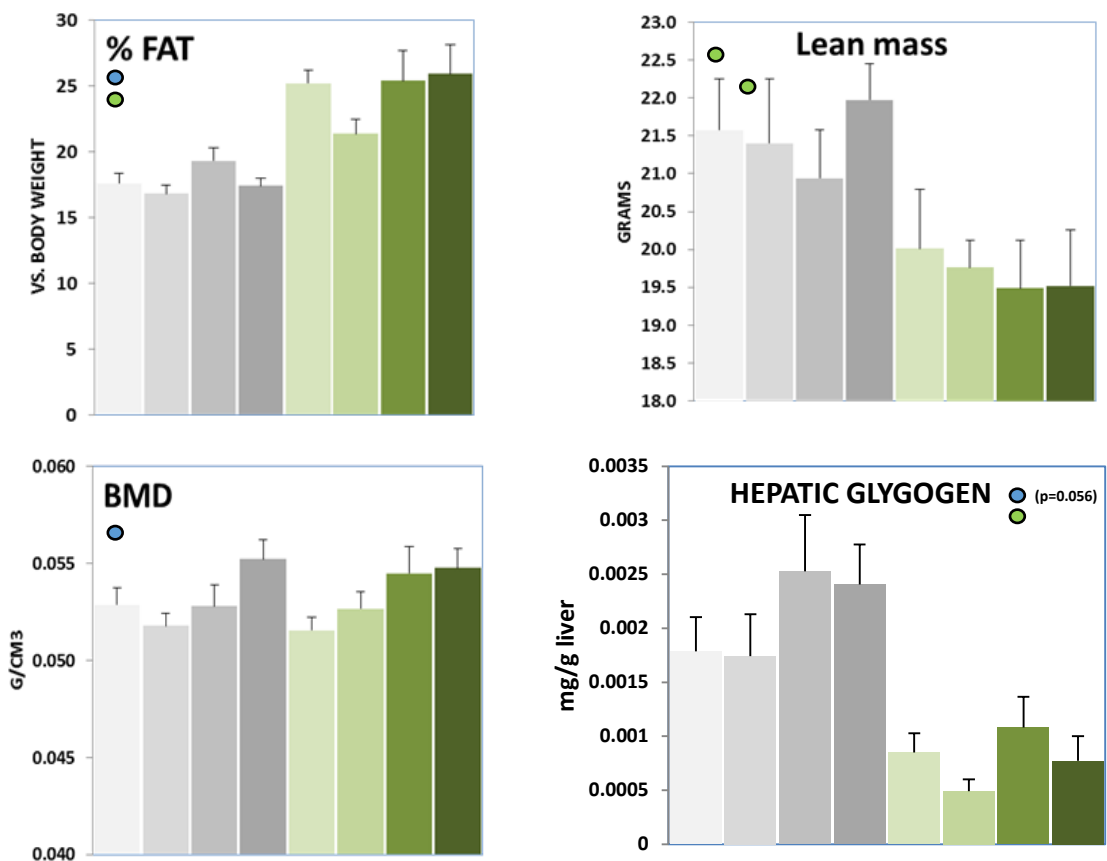
FIG 5



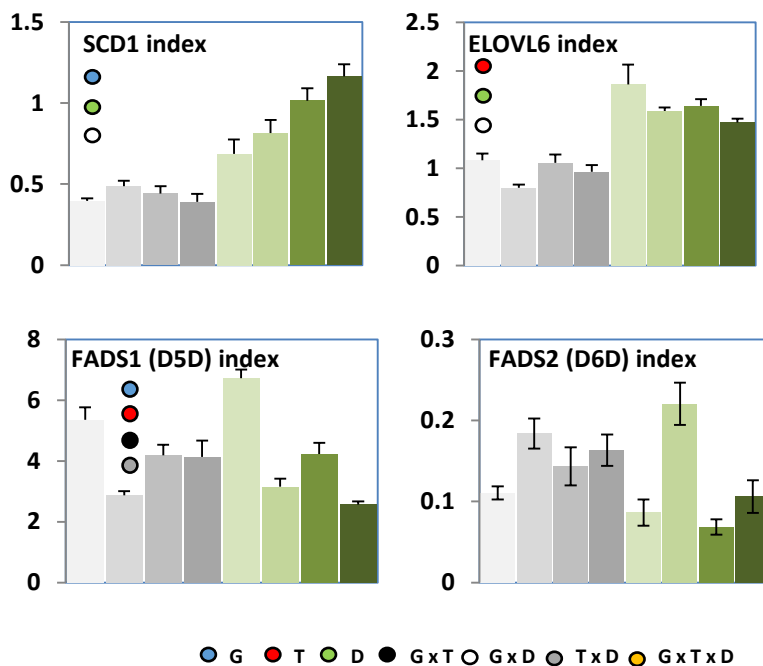
SFIG 1



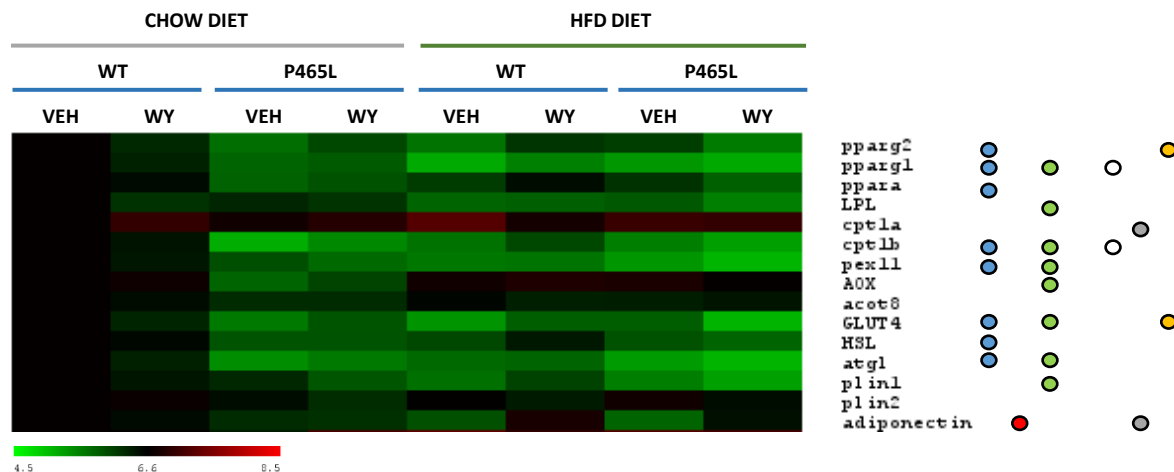
a



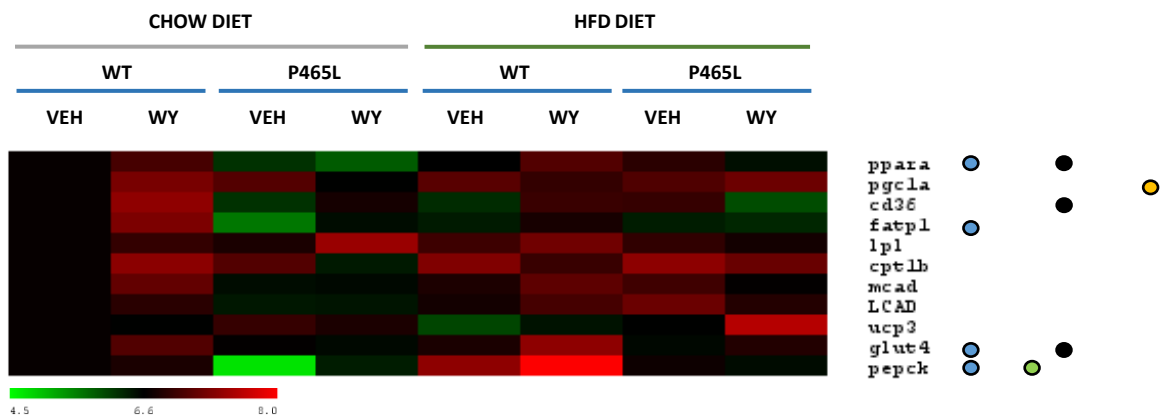
b



a
Gonadal WAT

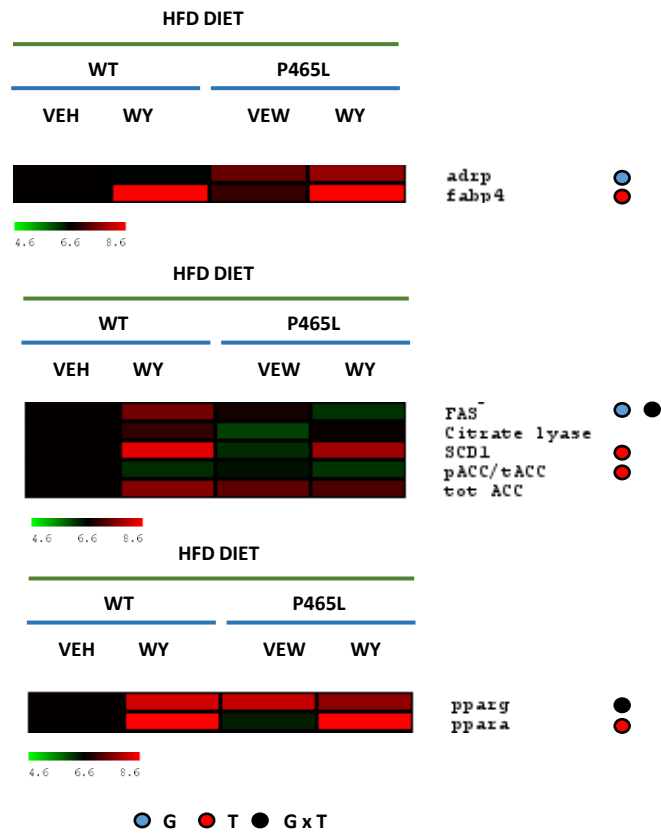


b
Skeletal Muscle

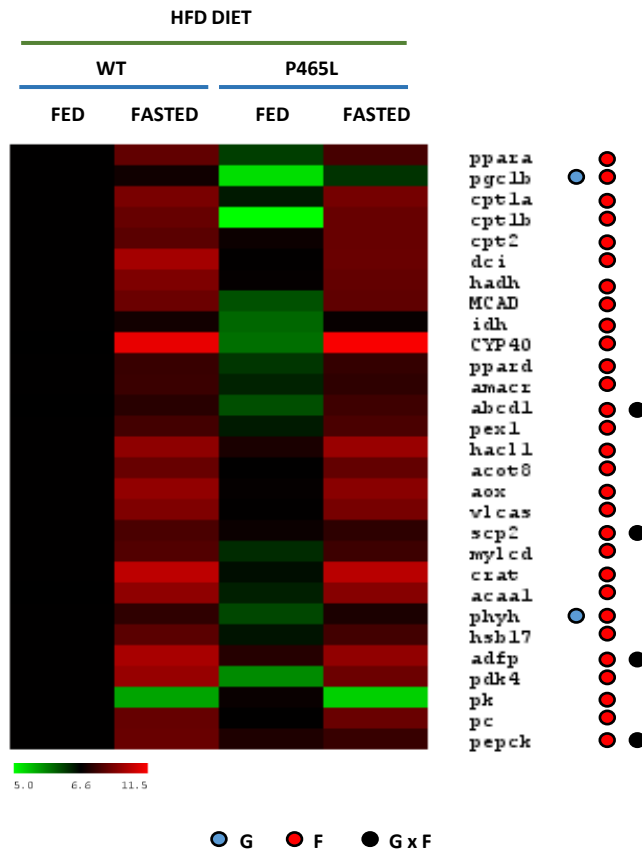


● G ● T ● D ● GxT ○ GxD ● TxD ● GxTxD

1 **a**



30 **b**



SUPPLEMENTAL FIGURE LEGENDS

SUPPLEMENTAL FIGURE 1. Blood biochemistry from P465L ppar γ mutant mice vs. WT mice fed chow or HFD for 3M in the fed and fasted state. Graphs represent the average of 5-8 mice per group \pm SEM analysed by ANOVA ($p < 0.05$). Different colour circles denote Genotype effect (blue), fasting (red), diet (green), interactive effect genotype x fasting (black), genotype x diet (white), diet x fasting (grey) and genotype x fasting x diet (orange).

SUPPLEMENTAL FIGURE 2. (a) Fat percentage, lean mass, bone mineral density (BMD) and Hepatic glycogen levels in P465L ppar γ mutant mice vs. WT mice fed chow or HFD with or without WY14643 (ip:25mg/kg). (b) Calculated SCD1, ELOVL6 and FADS1-2 ratio from data shown in Fig2b. Graphs represent the average of 5-8 (b) mice per group \pm SEM and analysed by ANOVA ($p < 0.05$). Different colour circles denote Genotype effect (blue), treatment (red), diet (green), interactive effect genotype x treatment (black), genotype x diet (white), diet x treatment (grey) and genotype x treatment x diet (orange).

SUPPLEMENTAL FIGURE 3. (a) Gene expression in gonadal adipose tissue (a) and skeletal muscle (b) is shown as log₂ conversions of average gene expression data relative to control ($\log_2 100 = 6.6$). Magnitude > 6.6 and < 6.6 denotes up- and downregulation, respectively, compared with WT, chow fed controls. (b) Hepatic levels of glycogen. Graphs represent the average of 7-8 mice per group \pm SEM and analysed by ANOVA ($p < 0.05$). Different colour circles denote Genotype effect (blue), treatment (red), diet (green), interactive effect genotype x treatment (black), genotype x diet (white), diet x treatment (grey) and genotype x treatment x diet (orange).

SUPPLEMENTAL FIGURE 4. (a) Expression of proteins involved in lipid droplet scaffolding, de novo lipogenesis and the transcription factors ppar γ and ppar α (b) Expression of genes relevant for liver metabolism from P465L ppar γ mutant mice vs. WT mice fed HFD for 12w in the fed and fasted state is shown as log₂ conversions of average gene expression data relative to control ($\log_2 100 = 6.6$). Magnitude > 6.6 and < 6.6 denotes up- and downregulation, respectively, compared with WT, HFD fed controls. Graphs represent the average of 6-8 mice per group \pm SEM and analysed by ANOVA ($p < 0.05$). Different colour circles denote Genotype effect (blue), fasting (red), and interactive effect genotype x fasting (black).